

**TRACTION CHARACTERISTICS OF A SHORTENED LAVAL NOZZLE WITH A BELL-SHAPED NOZZLE***Institute of Technical Mechanics**of the National Academy of Sciences of Ukraine and the State Space Agency of Ukraine,  
st. Leshko-Popelya, 15, 49005, Dnipro, Ukraine; e-mail: np-2006@ukr.net*

Наведено результати дослідження тягових характеристик надзвукового сопла нетрадиційної форми у вигляді укороченого сопла Лавалю з насадком дзвоноподібної форми. Така форма сопла може застосовуватися під час створення щільних компоновок багатоступеневих ракет. Дослідження проводилося з використанням програмного комплексу «ANSYS» у тривимірній постановці. Верифікацію використаних методичних підходів до числового розрахунку складної відривної течії газу було проведено попереднім дослідженням картини течії у подібному соплі. Окремі результати точних розрахунків порівнювалися з результатами експериментальних досліджень, проведених в Інституті технічної механіки Національної академії наук України і Державного космічного агентства України під час продування холодним повітрям моделі подібного укороченого сопла з дзвоноподібним насадком.

У цьому дослідженні були деталізовані особливості відривної течії газу в насадку сферичної форми, який був приєднаний (на кутовій точці) до укороченого надзвукового сопла Лавалю конічної форми. Було встановлено, що характер відривної течії в насадку залежить від ступеня розширення потоку (тиску на вході в сопло) з укороченого сопла. При відносно низькому тиску на вході в сопло в насадку спостерігається розвинена відривна зона (між кордоном струменя і стінкою насадка) з дозвуковим потоком із зовнішнього середовища, що формує практично постійний статичний тиск від перерізу входу в насадок до його зрізу. При тиску на вході в сопло, коли вільна межа струменя, що витікає з укороченого сопла, примикає до стінки насадка, статичний тиск у насадці практично лінійно змінюється по довжині насадка від кутової точки з мінімальним тиском до зрізу сопла. Залежність тяги сопла з насадком від тиску на вході в сопло нелінійна. Зі збільшенням тиску перед соплом (або зменшенням зовнішнього тиску) вплив зовнішнього середовища на тягу сопла з насадком зменшується. Показано, що в «земних умовах» тяга сопла з насадком перевищує тягу профільованого сопла з тим самим геометричним ступенем розширення (внаслідок «входу» атмосфери в насадок). В умовах вакууму тяга укороченого сопла з насадком на 8 % менше тяги профільованого сопла Лавалю.

**Ключові слова:** укорочене надзвукове сопло, дзвоноподібний насадок, розподіл статичного тиску, тягова характеристика сопла, тиск зовнішнього середовища.

This paper presents the results of a thrust performance study of an unconventionally shaped supersonic nozzle in the form of a truncated Laval nozzle with a bell-shaped tip. This nozzle shape may be used in the development of compact layouts of multistage rockets. The study was carried out using the ANSYS software package in a 3D formulation. The methodological approaches to the numerical calculation of a complex separated gas flow used in this study were verified in a previous study of the flow pattern in similar nozzle. Some results of exact calculations were compared with the results of experimental studies carried out at the Institute of Technical mechanics of the National Academy of Sciences of Ukraine and the State Space Agency of Ukraine for a model of a similar truncated nozzle with a bell-shaped tip blown with a cold air.

This study detailed the features of the separated gas flow in a spherical tip connected (at the corner point) to a truncated supersonic Laval nozzle of conical shape. It was found that the pattern of the separated flow in the tip depends on the nozzle flow expansion degree (nozzle inlet pressure). At a relatively low nozzle inlet pressure, a developed separation zone is observed in the nozzle tip (between the jet boundary and the nozzle wall) with a subsonic flow from the external environment, which forms an almost constant static pressure from the tip inlet cross-section to the tip exit. At a nozzle inlet pressure at which the free boundary of the jet flowing from the truncated nozzle adjoins the nozzle wall, the static pressure in the tip varies almost linearly along the tip length from the corner point with the minimum pressure to the tip exit. The dependence of the thrust of a tipped nozzle on the nozzle inlet pressure is nonlinear. As the pressure upstream of the nozzle increases (or the ambient pressure decreases), the effect of the external environment on the tipped-nozzle thrust diminishes. It is shown that under "terrestrial conditions" the thrust of a truncated nozzle with a tip exceeds the thrust of a profiled nozzle with the same geometric expansion degree (due to the atmosphere "entering" the tip). Under "vacuum" conditions, the former is 8% less than the latter.

**Keywords:** truncated supersonic nozzle, bell-shaped tip, static pressure distribution, nozzle thrust characteristic, ambient pressure.

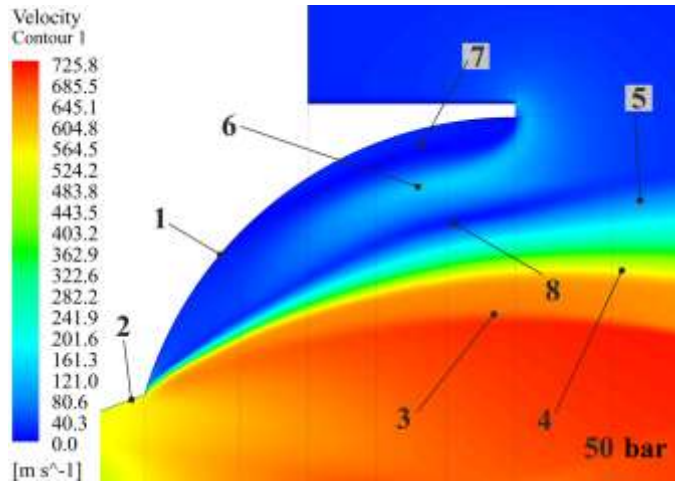
**Introduction.** In [1], the gas flow in a shortened Laval nozzle with a bell-shaped (spherical) tip was studied. A significant difference was shown between the flow in a nozzle with a packing and the flow in a Laval nozzle profiled along the

streamline of the same geometric degree of expansion, but without a packing. The existence of developed separation zones in the tip behind the corner point of the shortened nozzle exit (the transition of the nozzle wall into the tipping wall) has been established. It was found that the nature of the flow in the nozzle significantly depends on the total pressure of the gas flow in front of the nozzle (i.e., the degree of expansion of the flow in the nozzle). Some results of exact calculations (using the software package "ANSYS") were verified by the results of experimental studies of such a shortened nozzle characteristics [2]. Analysis of the similar studies results [3 – 6] (using software systems for solving the Navier–Stokes equations) also showed the adequacy of the models chosen in this work (viscosity, turbulence, etc.) for calculating the flow in a shortened Laval nozzle with a tip that causes separation of the gas jet flowing from the shortened nozzle at the nozzle wall.

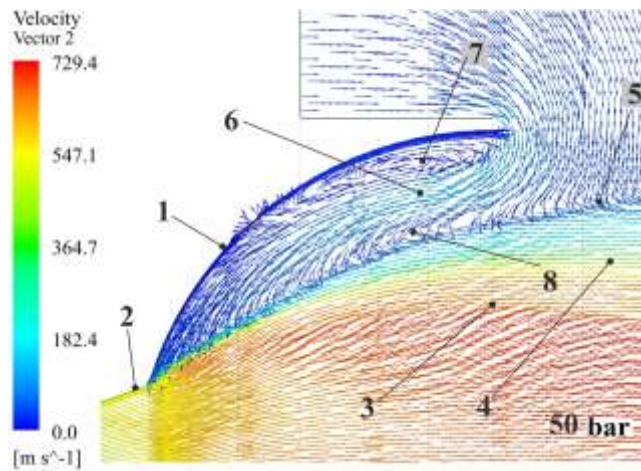
**The purpose of this work** is to investigate the power characteristics of the flow in nozzle with the bell-shaped tip.

**Main part.** In this work, using the same approach [1] (in the choice of the initial flow model, characteristic initial parameters, computational grid, restrictions on the process of establishment and convergence of the final results of the calculation, etc.), we studied in detail the power characteristics of the flow in a bell-shaped tip: pressure distributions on the wall of the nozzle and the traction characteristics of the nozzle with the tip.

Figure 1, a) shows the Mach number distribution field in the gas flow in a bell-shaped nozzle 1 behind the shortened supersonic Laval nozzle 2 exit at a nozzle inlet pressure of 50 bar ( $50 \cdot 10^5 \text{ N/m}^2$ ). The wave structure of a supersonic jet behind the nozzle exit is similar to the structure of a jet flowing into a flooded space [7]. Two hanging shocks 3 and 4 (the last has intensity less than 3) are observed in the jet. Such a feature of a supersonic jet flowing out of a nozzle tip distinguishes it from a jet flowing out of a Laval nozzle without a tip, where the hanging shock borders on the free jet boundary layer flowing out of the nozzle. Behind the shock 4, the velocity (in the cross section) equalizes (in magnitude and direction) with the velocity near the free boundary 5 of the jet (see Fig. 1, b)). Between the free jet boundary 5 and nozzle wall 1, there is a developed separation zone with a pronounced subsonic flow 6 and two large-scale differently directed vortices 7 and 8 (see Fig. 1, a) and 1, b)). Vortex 7 occurs between flow 6 and nozzle wall 1. Vortex 8 arises between flow 6 and the free jet boundary 5. At the free jet boundary 5 along the entire length of the nozzle tip, there is gas inflow from the separation zone of the tip into the jet. The intensity of penetration of the external flow into the free boundary layer of the jet varies along the tip length, changing its character beyond the tip exit, where mass transfer occurs, which is typical for the interaction of a free jet with the surrounding stationary medium.



a)



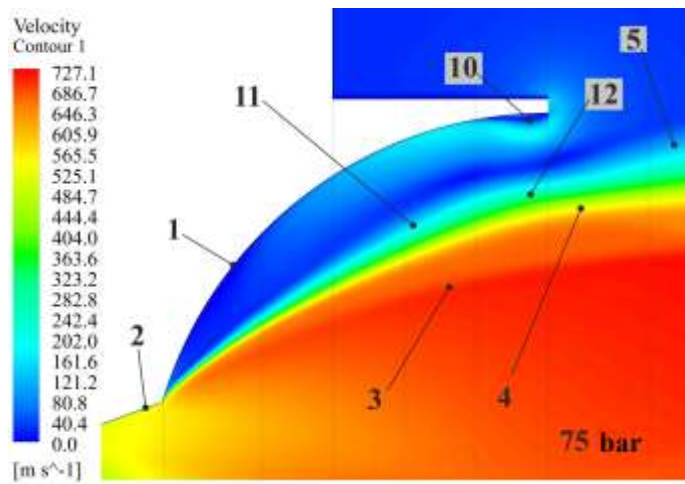
b)

1 – tip wall; 2 – wall of a shortened nozzle; 3 – hanging shock in the jet behind the shortened nozzle exit; 4 – hanging shock of lower intensity; 5 – free jet boundary; 6 – the flow of the external environment into the tip; 7 – near-wall toroidal vortex; 8 – free toroidal vortex

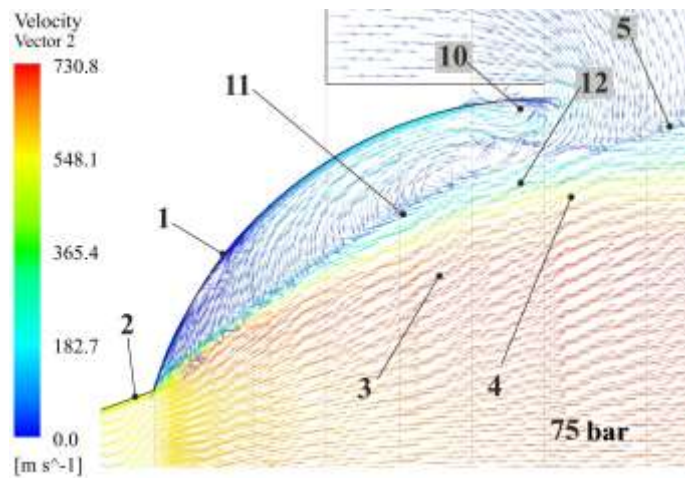
a) the distribution of Mach numbers in the gas flow behind the shortened nozzle exit; b) the distribution of velocity vectors in the gas flow behind the shortened nozzle exit.

Fig. 1 – Flow in the bell-shaped tip of a shortened Laval nozzle at a nozzle inlet pressure of 50 bar

Figure 2 shows the velocity field (Fig. 2, a)) and the velocity vector field (Fig. 2, b)) at a pressure of 75 bar at the nozzle inlet. The transverse dimensions of the jet (the boundary of the jet in the section of the tip exit) flowing out of the shortened Laval nozzle 2 increases (compared to the flow at  $p_0=50$  bar) by 15 %. In this case, the relative transverse dimensions of hanging shocks 3 and 4 increase by 20 %. This is explained by an increase in the non-design degree of the jet flowing from the shortened nozzle.



a)



b)

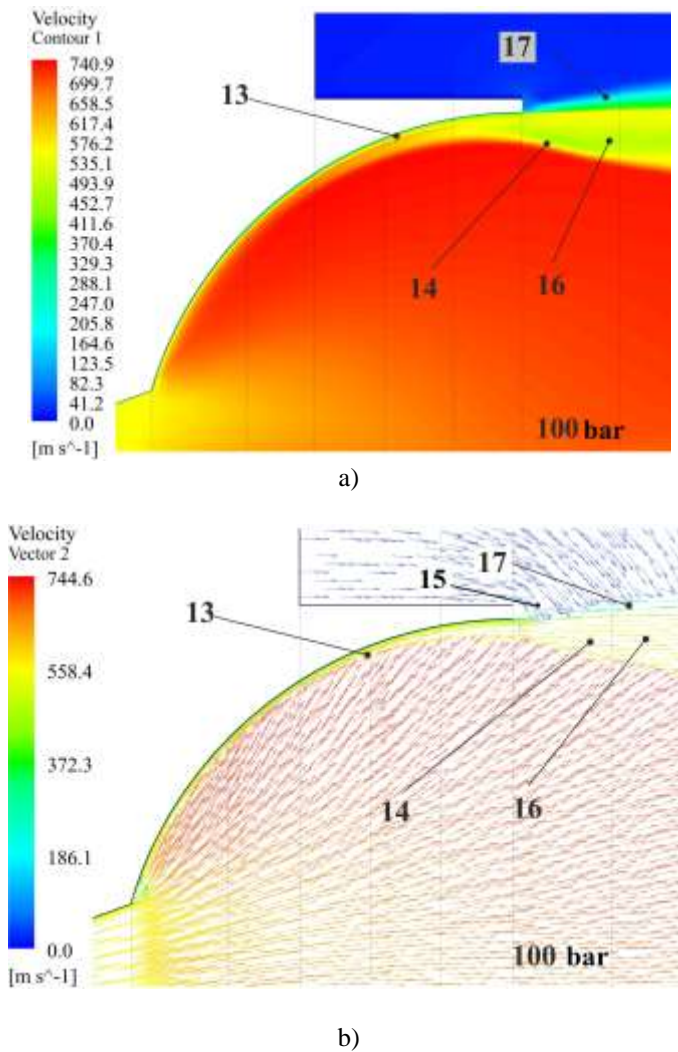
1 – nozzle wall; 2 – wall of a shortened nozzle; 3 – hanging shock in the jet behind the cut of the shortened nozzle; 4 – hanging shock of lower intensity; 5 – free jet boundary, 10 – near-wall toroidal vortex; 11 – free toroidal vortex; 12 – free jet boundary  
a) velocity distribution in the gas flow; b) distribution of velocity vectors.

Fig. 2 – Flow in the bell-shaped tip of a shortened Laval nozzle at a nozzle inlet pressure of 75 bar

The flow in the separation zone between the free jet boundary and the nozzle wall changes its character. Subsonic flow 6 is not observed in the flow (see Fig. 1). At the same time, a relatively small-scale vortex 10 appears at the exit edge of the tip, caused by local inflow of the external flow into the tip to its wall. In other words, an intense toroidal vortex appears near the exit edge of the tip. This vortex manifests itself in the static pressure distribution as a local short-range pressure increase. In the separated flow, one large-scale vortex 11 (see Fig. 2) of relatively high intensity with reduced pressure (in the region of the indicated vortex) prevails on the tip wall. It should be noted that there is a distortion in the shape of the free

jet boundary 12 near the tip exit (local decrease in the diameter of the free boundary) caused by toroidal vortex 10 (see Fig. 2, a)).

At a pressure  $p_0=100$  bar, the separation zone between the jet boundary and the tip wall degenerates into a developed boundary layer 13 between the hanging shock 14 originating at the exit edge of the shortened nozzle and the tip wall (see Fig. 3, a)).

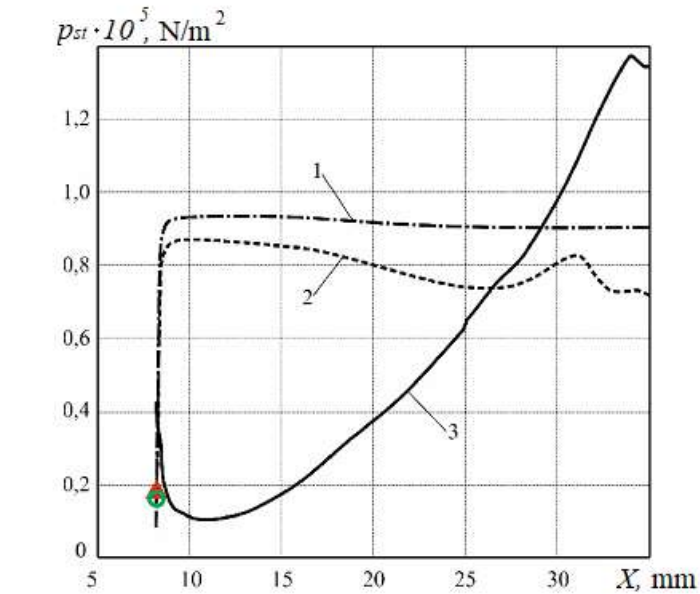


a) speed distribution; b) distribution of velocity vectors

Fig. 3 – Flow in the bell-shaped tip of a shortened Laval nozzle at a nozzle inlet pressure of 100 bar

Within the tip, the viscosity forces press the hanging shock 14 against the wall of the tip, thus reducing the thickness of the layer 13. In this case, secondary hanging shock is not observed, as in the case of a developed separated flow in the tip (Fig. 1, a) and 2, a)). Near the tip exit, it is observed from the break of the hanging shock 14. This can be explained by the influence of the environment on the relatively low-velocity flow behind the hanging shock 14. In fig. 3, b), this influence manifests itself in the intense inflow form of the external flow to the jet boundary

at the tip exit (the magnitude and direction of vectors 15). The incoming low-velocity flow causes flow 16 (see Fig. 3, a)) with a reduced velocity relative to the flow behind the hanging shock 14 in its central part, between the hanging shock 14 and the free jet boundary 17.



1 – 50 bar; 2 – 75 bar; 3 – 100 bar – exact calculation  
 $\Delta$  (0.186 bar) – one-dimensional calculation of the Prandtl-Meier flow behind the cut of the shortened nozzle;  $\circ$  (0.181 bar) – one-dimensional calculation of flow expansion in a profiled Laval nozzle

Fig. 4 – Static pressure distribution in a bell nozzle at nozzle inlet pressure

Figure 4 shows the distribution of static pressure in a bell-shaped tip at various nozzle inlet pressures and one-dimensional calculation of pressure at the corner point (at  $p_0=100$  bar).

Here, line 1 denotes the (exact) calculated dependence of the static pressure in the nozzle on the longitudinal coordinate (at a total pressure in front of the nozzle of 50 bar ( $50 \cdot 10^5 \text{ N/m}^2$ ) and a pressure of the medium surrounding the nozzle of 1 bar). The longitudinal coordinate was counted from the critical section of the shortened nozzle ( $X=0$  mm) to the nozzle exit ( $X=35$  mm). The corner point (transition of the nozzle into the tip) of the nozzle is located at a distance of 8.15 mm from the critical section of the shortened nozzle. At the corner point of the nozzle, the pressure drops in expansion waves (Prandtl–Meier flows) from the pressure at the tip exit to the pressure at the maximum angle of the gas flow at the corner point. Then the pressure rises sharply to a value of 0.93 bar at the beginning of the separation zone. Then the pressure decreases slightly (to 0.91 bar in the middle of the tip) and remains almost constant downstream to the shear of the tip. In this region, the flow pattern (see Fig. 1) shows a local vortex zone 7 with a toroidal structure.

At  $p_0=75$  bar (line 2) the distribution of static pressure in the tip is similar (but with peculiarities) to the distribution at  $p_0=50$  bar (line 1). At the beginning of the separation zone, the pressure from the corner point of the nozzle (with the Prandtl–Meier flow) increases to a value of 0.85 bar. However, downstream the pressure drops with a larger gradient (than at  $p_0=50$  bar) to a value of 0.76 bar at a distance of 27 mm from the exit of the shortened nozzle. This is explained by the increased

velocity of the subsonic gas flow in the large-scale toroidal vortex 11 (see Fig. 2). The local inflow of a jet from the surrounding space onto the nozzle wall, caused by a local toroidal vortex 10 (Fig. 2), causes a secondary increase in pressure to a value of 0.83 bar at a distance (upstream) of 3 mm, counting from the tip exit. Further downstream, the pressure drops again to 0.72 bar. In this case, there is a local slight increase in pressure at the tip exit, caused by the initial stage of the influence of the gas jet leaking onto the nozzle wall, flowing from the shortened Laval nozzle. With an increase in pressure at the nozzle inlet and, as a result, a decrease in the size of the separation zone in the nozzle, the indicated local increase in pressure at the tip exit is more pronounced (at  $p_0 = 50$  bar, it is completely absent) and shifts downstream to the nozzle exit.

Line 3 (Fig. 4) indicates the distribution of static pressure in the tip at a pressure at the nozzle inlet of 100 bar. This pressure in front of the nozzle turned out to be critical for the existence of a separation zone behind the corner point of this shortened nozzle. In the pressure distribution just behind the corner point (at  $X=8.15$  mm) there is a sharp decrease in pressure in the Prandtl–Meyer flow to a value of 0.12 bar. Then there is an almost linear increase in pressure up to a value of 1.36 bar at the nozzle exit. It should be noted that the tip shear pressure exceeds the ambient pressure (1.0 bar). This is due to the intense inflow of the gas flow from the shortened nozzle to the wall of the tip at its exit. In the local area of inflow of the external medium to the wall at the nozzle exit ( $X=0.034$  m), there is an increase (“splash”) of the static pressure of a small extent up to a value of 1.38 bar. After the flow reversal in the Prandtl–Meyer flow at the corner entry point into the tip due to the spherical shape of the nozzle wall it flows at some angle to the nozzle wall at its exit, causing the indicated local increase in static pressure. The legitimacy of explaining this behavior of a jet flowing from a shortened nozzle is confirmed by an increase in the pressure growth gradient, starting from the middle of the nozzle to its exit (manifested in the violation of linearity in the dependence of the pressure distribution along the length of the nozzle).

The pressure behind the exit of the shortened nozzle (at the inlet corner point of the nozzle) was calculated using one-dimensional models of flow expansion in the Prandtl–Meyer flow and by gas-dynamic functions of flow expansion in the Laval nozzle with the same (as in the nozzle) geometric degree of flow expansion ( $q(\lambda_a)=0.032$ ,  $\lambda_a=V_a/a_{cr}$ , where  $a_{cr}$  is the critical flow velocity,  $V_a$  is the velocity at the tip exit area) of gas in the nozzle (from the critical section with a diameter of 10 mm to the outlet section equal to the outlet section of a bell-shaped nozzle with a diameter of 56 mm).

In the one-dimensional calculation of the Prandtl–Meier flow, the flow turned at the corner point of entry into the bell-shaped tip by an angle  $\delta = \alpha + \varphi - \frac{\pi}{2}$ ,

where  $\alpha = \arcsin \frac{1}{M}$  is the propagation angle of weak perturbations;  $M = \frac{v}{a}$  – flow Mach number;  $v$  – flow rate;  $a$  is the local flow sound velocity. The polar angle of the flow reversal in the refraction wave fan is determined from the relation  $\varphi = \sqrt{\frac{k+1}{k-1}} \arcsin \sqrt{\frac{k-1}{2}(\lambda^2 - 1)}$ , where  $k$  is the adiabatic index of the gas flow.



The reduced velocity  $\lambda$  is related to the Mach number by the relation

$$\lambda = \frac{v}{a_{cr}} = \frac{M \sqrt{\frac{k+1}{2}}}{\sqrt{1 + \frac{k-1}{2} M^2}}.$$

The total angle of flow rotation at the corner point was assumed to be  $\delta_\Sigma = \delta_n + \delta_n = 77^\circ$ , where  $\delta_n = 20^\circ$  is the angle of flow rotation in the shortened nozzle;  $\delta_n = 57^\circ$  is the angle of flow rotation at the corner point of the tip. For this angle of rotation, the calculated value of the relative static flow pressure

$$\frac{p}{p_0} = \left(1 + \frac{k-1}{k+1} \lambda_\Sigma^2\right)^{\frac{k}{k-1}} \text{ was } 0.186 \cdot 10^{-2}, \text{ i.e. the absolute value of the static pressure}$$

after the flow reversal at the corner point of the nozzle was 0.186 bar, where  $\lambda_\Sigma$  is the reduced velocity in the fan of expansion waves on the characteristic of the angle. In Fig. 4 this point is indicated by a triangular icon.

When calculating the static pressure at the section of a shortened Laval nozzle using gas-dynamic functions, it was assumed that the flow at the nozzle corner point expands to a relative value

$$q(\lambda_a) = \frac{p_a v_a}{p_{cr} v_{cr}} = \left(\frac{k+1}{2}\right)^{\frac{1}{k-1}} \cdot \left(1 - \frac{k-1}{k+1} \lambda_{anoz}^2\right)^{\frac{1}{k-1}} \cdot \lambda_{anoz},$$

where  $\lambda_{anoz}$  is the reduced velocity corresponding to the tip exit area (diameter – 56 mm) with a geometric degree of flow expansion equal to  $q(\lambda_a) = 0.032$ ;  $p_a$ ,  $v_a$ ,  $p_{cr}$ ,  $v_{cr}$  are the pressure and velocity at the tip exit area and the critical section, respectively. For this value of the flow expansion degree in the tip, the relative static

pressure is  $\frac{p_{anoz}}{p_0} = \left(1 - \frac{k-1}{k+1} \lambda_{anoz}^2\right)^{\frac{k}{k-1}}$ . The absolute value of  $p_{anoz} = 0.181$  bar.

In Fig. 6 this value is indicated by a round icon (in the section of 8.15 mm, in which the nozzle corner point is located).

The calculated points (according to the one-dimensional theory) on the graph in Fig. 6 are “attached” to the section ( $X=8.15$  mm), in which the transition corner point of the shortened Laval nozzle exit to the tip is located. From Fig. 4 it can be seen that at the specified corner point there is a local flow over-expansion of insignificant length (from 9 to 13 mm), where the minimum static pressure is 0.12 bar. Such a local behavior of the flow at the corner point is not taken into account by calculations based on the one-dimensional theory. Nevertheless, one can note a satisfactory agreement between the results of exact calculations of the static pressure behind the corner point of the nozzle (graph line) and the results obtained using the one-dimensional theory (points marked with icons).

Downstream to the tip exit, the static pressure increases almost linearly to 1.35 bar, which corresponds to the geometric expansion ratio of the flow  $q(\lambda)=0.1507$ , according to one-dimensional theory calculation. The geometric ex-

pansion ratio of the Laval nozzle is  $q_{Ln} = \frac{F_{crLn}}{F_{aLn}} = \left(\frac{10}{17.3}\right)^2 = 0.334$ , where  $F_{crLn}$

is the critical section area of the Laval nozzle;  $F_{aLn}$  – Laval nozzle exit area. The



expansion degree of the shortened nozzle is  $q_{anoz} = \frac{F_{crLn}}{F_{anoz}} = \left(\frac{10}{56}\right)^2 = 0.0319$  (here

$F_{anoz}$  – nozzle exit area). For the value  $q(\lambda) = \frac{q_{Ln} - q_{anoz}}{2} = 0.151$ , the value  $\pi(\lambda) = 0.0136$  or an absolute pressure is 1.36 bar. This pressure is practically equal to the exact calculation (1.35 bar).

Thus, in approximate calculations of the static pressure in the tip in the case when the free boundary of the jet flowing from the shortened nozzle adjoins the tip wall, the relations of the one-dimensional theory in the above interpretation can be used to determine the average value  $q(\lambda)$  of the bell-shaped tip.

Figure 5 shows the distribution of static pressure in the nozzle at external pressure  $p_0 = 0.1$  bar and nozzle inlet pressure of 50 bar (line 1); 75 bar (line 2); 100 bar (line 3).

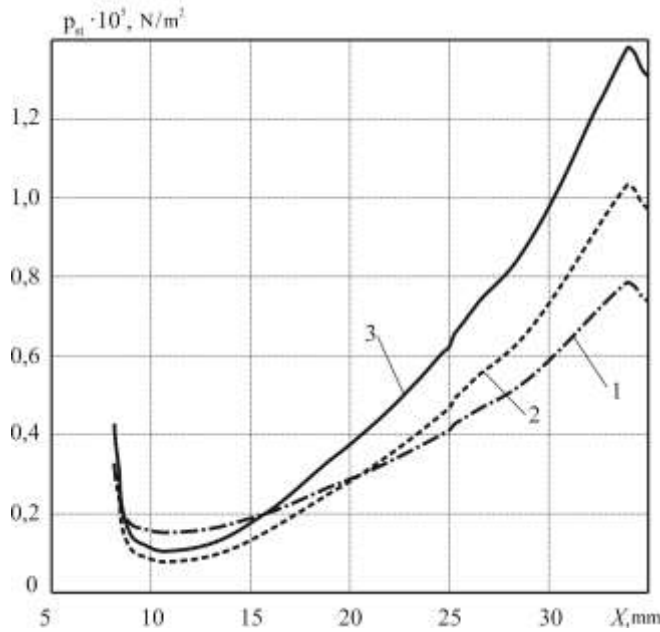
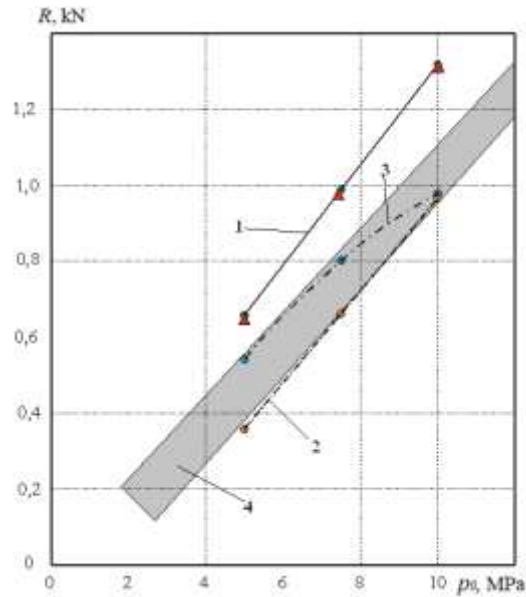


Fig. 5 – Static pressure distribution in the bell-shaped tip at external pressure  $p_0 = 0.1$  bar and nozzle inlet pressure  $p_0$ : line 1 – 50 bar; 2 – 75 bar; 3 – 100 bar

In this case, the flow in the tip is not separated, i.e. similar to the flow considered above at  $p_0 = 100$  bar and  $p_{ext} = 1$  bar. At different pressures (50, 75, 100 bar) at the nozzle inlet, the distribution of static pressure in the tip has the same character: a drop at the corner point of the nozzle (transition from the nozzle to the tip) and almost linear increase to the tip exit. At high pressures at the nozzle inlet (100, 75 bar), the static pressure in the nozzle changes almost in proportion to the pressure at the nozzle inlet. At low inlet pressure, this dependence changes disproportionately: 10 % less at a pressure of 50 bar. This is explained by the origin of a toroidal vortex at the beginning of separation of the flow boundary from the tip wall. With a further decrease in pressure at the nozzle inlet, the separation zone increases in size, capturing the whole tip.

Figure 6 shows the dependence of thrust on the total pressure in front of the nozzle. Here, lines 1 and 2 indicate the results of numerical calculations of the

thrust of a profiled Laval nozzle (the same geometric expansion ratio as that of a nozzle with a tip) using the ANSYS package.



1 – “empty” thrust of a profiled Laval nozzle with a geometric expansion ratio of 31.4; 2 – “earthly” thrust of the same nozzle; 3 – accurate calculation of the thrust of a shortened nozzle with a bell-shaped tip; 4 – field of experimental values of thrust of a shortened nozzle with a bell-shaped nozzle; triangular symbols indicate the thrust dependence of the Laval nozzle of the same degree of expansion (0.0319), calculated according to the one-dimensional theory.

Fig. 6 – Dependence of thrust on the total pressure at the nozzle inlet

In this case, line 1 is the integral of the static pressure forces along the nozzle contour, where round symbols are the results of calculations at different pressures in front of the nozzle. Line 2 is the integral over the contour minus the counteraction of the external pressure  $p_H F_a$ , where  $p_H$  – the external pressure of the environment,  $F_a$  – the area of the nozzle exit. The triangular symbols (almost lying on line 1) indicate the results of calculations according to the one-dimensional theory of “void” thrust (at  $p_H = 0$ ) of a profiled Laval nozzle with a geometric expansion ratio of 0.0319. The results of exact calculations of the thrust of the Laval nozzle practically coincided with the results of calculations according to the one-dimensional theory. Approximating (calculation results) polynomials of dependences of the profiled Laval nozzle thrust on the pressure in front of the nozzle are obtained in the following form: exact calculations of the thrust  $R_{ex} = 0.1318 p_0 + 0.0002$ ; calculations according to one-dimensional theory  $R_{onedim} = 0.1311 p_0$ .

The results of the above comparisons (exact and one-dimensional calculations) can serve as an additional substantiation of the result reliability, verification of the calculation results, obtained when calculating the thrust characteristics of the shortened nozzle with a bell-shaped tip considered in this case (“non-traditional”).

The dependence of the shortened Laval nozzle thrust with a bell-shaped tip has a different character (see line 3 in Fig. 6). Shaded field 4 in Fig. 6 is the results of experimental studies of a shortened nozzle with a bell-shaped tip № 6 [2]. Flow patterns in a shortened nozzle with a nozzle were studied in [1].

In this case, the external pressure significantly affects the thrust characteristic of the nozzle with a tip. At a high pressure of the external environment ( $p_n = 1$  bar), it “penetrates” into the nozzle into the cavity bounded by the wall of the tip and the boundary of the jet flowing out of the shortened nozzle with separation from the edge of the outlet section of the shortened nozzle (see Fig. 1 and 2). In this case, a vortex flow occurs in this cavity with a pressure slightly lower than the ambient pressure (0.91 bar at the nozzle inlet pressure of 50 bar). With an increase in pressure in front of the nozzle (in our case, up to 75 bar), the jet flowing out of the shortened nozzle increases in diameter, filling the indicated zone between the jet boundary and the wall of the tip. The pressure in this cavity decreases (to a value of 0.76 bar). In this case, the thrust of the nozzle with the tip also decreases compared to the case of a developed separated flow at a lower pressure in front of the nozzle. This occurs due to a decrease in the influence of the external environment (penetrating into the separation zone of the tip) on the thrust of the shortened nozzle with the tip.

The approximating polynomial thrust dependence for the nozzle with a tip on the total pressure at the nozzle inlet is obtained in the form:  $R_{noz} = -0.0079 p_0^2 + 0.2026 p_0 - 0.2752$ . In contrast to the dependence for a profiled Laval nozzle, this dependence is non-linear (for the above reasons).

The obtained approximating thrust dependences of a shortened nozzle with the studied type of bell-shaped tip on the pressure in front of the nozzle can be used for approximate calculations of the characteristics of a shortened nozzle with a similar tip in the design development of dense rocket layouts.

**Conclusions.** Using a verified approach in the choice of initial data for a numerical study (using the ANSYS package) of a separated flow in a shortened Laval nozzle with a bell-shaped tip, the pressure distribution on the wall and the thrust characteristics of the nozzle with a tip were determined.

The nature of the separated flow in the nozzle depends on the expansion degree of the flow from the shortened nozzle. At a relatively low pressure at the nozzle inlet, a developed separation zone is observed in the tip (between the jet boundary and the tip wall) with a counterflow from the external environment, which forms an almost constant static pressure from the corner point to the tip exit.

When the pressure changes large-scale toroidal vortex structures are formed in the nozzle separation zone, which results in a variable static pressure along the tip length.

Under “terrestrial” conditions, the thrust of a nozzle with a bell-shaped tip is higher than the thrust of a Laval nozzle profiled along the streamline (with the same geometric degree of expansion) without a tip, which is explained by the penetration of the external medium into the separation zone of the tip. The dependence of the thrust of the nozzle with a tip on the pressure at the nozzle inlet is non-linear.

In “empty” conditions, the thrust of a shortened nozzle with a tip is 8 % less than the thrust of a Laval nozzle profiled along the streamline with the same geometric expansion degree.

1. Ihnatiev O., Pryadko N., Strelnikov G., Ternova K. Gas flow in a short Laval nozzle with a bell-shaped nozzle. Technical mechanics. 2022. № 2. P. 39–46. <https://doi.org/10.15407/itm2022.02.039>
2. Strelnikov G. A. Adjustable supersonic nozzles of small length (rus). Dnepropetrovsk, ed. DGU 1993. 191 p.

3. *N Lenin Rakesh* Analysis of flow of nozzle by using ANSYS. Journal of mechanics of continua and mathematical sciences. 2019. Vol. 1. P. 1–8. <https://doi.org/10.26782/jmcms.spl.2019.08.00088>
4. *Yashraj Asthana* CFD Analysis of Different Types of Advanced Rocket Nozzles in Ansys. International Journal of Advancements in Technology. 2022. Vol. 13. Iss. 2. P. 1–6.
5. *G. Susheel Narayan, Vikky Chobey, P. Mani Kiran, Mihir Baranwal* A research paper on analysis of de-laval nozzle on Ansys Workbench. International Research Journal of engineering and Technology (IRJET). 2019. Vol. 6. Iss. 11. P. 471–477.
6. *Muhammad Waqas Khalid, Muhammad Ahsan* Computational Fluid Dynamics Analysis of Compressible Flow Through a Converging-Diverging Nozzle using the k- $\epsilon$  Turbulence Model. Engineering, Technology & Applied Science Research. 2020. Vol. 10. №1. P. 5180–5185. <https://doi.org/10.48084/etasr.3140>
7. *Abramovich G. N.* Applied gas dynamics (rus). Edition 5. M.: "Nauka". 1991. 600 p.

Received on July 25, 2022,  
in final form on Oktober 10, 2022